Int. J. Electrochem. Sci., 11 **(2016)** 9100 – 9109, doi: 10.20964/2016.11.12

International Journal of
ELECTROCHEMICAL
SCIENCE
www.electrochemsci.org

Comparing the Air Flow Distribution Qualities Among Three Different Air Flow Path Configurations for Tubular Solid Oxide Fuel Cell Stacks

Zidong Yu[1,2,*], *Yu Xu*[2], *Biao Hu*[2], *Shengji Liu*[1,*], *Xinyi Zhang*[2]

[1] School of Automobile and Traffic Engineering, Jiangsu University, Zhenjiang, Jiangsu 212013, China;
[2] School of Energy and Power Engineering, Jiangsu University of Science and Technology, Zhenjiang, Jiangsu 212003, China.
[*]E-mail: yuzidong@just.edu.cn

Received: 21 July 2016 / *Accepted:* 2 September 2016 / *Published:* 10 October 2016

In this paper, the air flow distribution quality within a conventional tubular solid oxide fuel cell (T-SOFC) stack air flow path structure was analyzed by 3D calculating fluid dynamics (CFD) simulating. The air flow field within the T-SOFC stack was of a typically turbulence characteristic. Both air flow distribution qualities among 36 T-SOFC units in stack level and over each T-SOFCs unit surface within the T-SOFC stacks with different air flow manifold configuration designs, such as 1in1out-line, 1in1out-Z, and 2in2out-Z type, were carefully compared through 3D simulation. 2in2out-Z type air flow path structure was concluded to be a more suitable chooses for T-SOFC stack, because its smaller variation of x-velocity at each main plane than that in other type air flow path structures.

Keywords: Tubular SOFC stack, air flow distributing path optimization, turbulence flow characteristic.

1. INTRODUCTION

Solid oxide fuel cell (SOFC)is considered to be a promising power generation devices due to its fuel flexibility from various renewable sources, high conversion efficiency, the absence of combustion and low environmental impact [1-5]. Generally, the SOFC unit performance was considered as the fundamental influent factor for SOFC stack. However, many high performance cell units are always combined to a bad stack performance and low duration lifetime [6]. Overloading of the single zones within a cell or repeating unit itself can result in failure and subsequent progressive degradation of the stack as a whole. Thus, even loading and keeping current induced degradation processes constantly distributed throughout the stack are essential to extend the overall stack lifetime [7]. The further

development of SOFCs faces the challenges to maximize the power density and minimize the unwanted temperature variation throughout the whole stack, which contributes to the thermal stress in different components [8, 9]. These will rely on the proper air flow path design to ensure high air flow distribution qualities within the stack.

In the past decade, more and more attentions had been paid on investigating proper stack structure designs to achieve high stack performance and overall lifetime [4, 10-13]. M. Peksen had coupled the CFD and computational solid mechanics model to simulate the heating-up process to achieve the induced thermal stress within a specific planar SOFC stack [4]. Y. P. Chyou et al. had developed a heat transfer models for the typical planar SOFC units with co-, counter and cross fuel & air arrangement pattern, and the air flow distribution was found to be a very important factor to determine both the temperature and electrochemical reaction distributions within a stack [14, 15]. Computer simulation had been employed by D. Yan et al. to test the planar SOFC stacks with external manifold and obtained the optimized parameters [16]. The effects of different rib shapes (i.e., rectangle and discrete cylinder) on the air flow distributions within the specific planar SOFC stacks had been numerically compared by 3D computational fluid dynamics (CFD) modeling [17, 18, 19]; and the planar stack using rectangular rib configuration for fuel side and discrete symmetric cylindrical rib configuration to construct air flow channels was concluded to be a suitable design for that type of planar SOFC stacks [18].

Conclusively, a suitable air flow manifold configuration design can not only feed air flow uniformly among the T-SOFC units and over each T-SOFC active cathode surface, but also can provide sufficient air flow to remove possible hot spots during performance. As reviewed above, CFD methods had been widely adopting to investigate the flow distributing characteristics within different planer SOFC stack designs and optimize the stack parameters. It was generally agreed to be an accurate and effective approach. However, as far as we know, there were rare reports on the 3D CFD analyzing and optimizing for 3D air flow path within the tubular solid oxide fuel cell (T-SOFC) stack designs.

In this paper, the air distribution characteristics within a convenient tubular SOFC stacks were figured out and assessed by the 3D CFD model developing and simulating. The air flow distributing qualities among 36 T-SOFC units in stack level and over each T-SOFC unit surface in single cell level were carefully analyzed to illustrate the practicable of the current used air flow path. Finally, the air flow distributions qualities within different air flow path configuration for T-SOFC stacks, such as, 1in1out-line, 1in1out-Z, and 2in2out-Z, were compared to achieve the optimized results.

2. CFD MODELING OF 3D AIR FLOW PATH WITHIN CONVENTIONAL T-STACKS

The sketch diagram of air flow path within a conventional T-SOFC stack was illustrated in Fig. 1a. 36 tubular SOFC units (i. e., diameter d=15 mm, length L=150 mm) were metrically connected with an interval 8 mm. The total active areas of all T-SOFC units within the stack was around,

$$S = 36\pi dL = 36\times 3.14\times 15\times 10^{-3}\times 150\times 10^{-3} = 0.254\ \mathrm{m}^2, \quad (1)$$

The configuration of conventional air flow path within this T-SOFC stack was indicated as

1in1out 'line-type' configuration. 1in1out meant two manifolds (inlet and outlet) were placed at the centers of the opposite surfaces, respectively. Their effects were feeding the air flows to each tubular SOFC unit, collecting exhaust gas and cooling the stack. For the case with average output current density j around 7000 A m^{-2}, effective utilization of air flow η_{O_2} around 20%, the mass flow rate at the manifold inlet can be evaluated as,

$$\dot{m}_{air} = \frac{jSM_{air}}{4F\eta_{O_2}\chi_{O_2}} \approx 0.00318 \text{ kg s}^{-1}, \quad (2)$$

Where F was the Faraday constant, equaled to the total electric column of one molar electrons. M_{O_2} was the molar mass of oxygen. χ_{O_2} was the mass fraction of oxygen within air mixture. Then the manifold inlet velocity can be conveniently evaluated as $u_{air} = \dot{m}_{air} / (\rho_{air} A_{in}) \approx 28.7 \text{ m s}^{-1}$. ρ_{air} was air mass density; $A_{in} = \pi r_{in}^2$ was the total areas of inlet manifold entrances. In current case, the radii of both inlet and outlet manifolds r_{in}=r_{out} were around 10 mm.

Mesh grid dividing was one of the most important steps to achieve proper 3D CFD calculating results within the complicated 3D air flow path of T-SOFC stacks. Enough hexagonal mesh elements around 1564276 were addred to the current 3D CFD air flow path model to ensure the accuracy. For this case, the Reynolds number within the inlet manifolds was high around 39295.3, which was of typical turbulent flow characteristic. The k-ε model was chosen for the turbulent flow field simulating.

Finally, the flow characteristics of air fluid distribution within the conventional T-stack would be figured out by the 3D CFD approach using software Fluent with a tolerance 1×10^{-5}. The detailed process of 3D model developing, meshing and simulating processes could be found in many previous papers [18, 20].

For carefully getting the air flow distributing characteristics and qualities within T-SOFC stack, six *y*-*z* main planes 'plane *i*(*i*=1, 2…6)' along *x* direction were indexed in Fig. 1b. Each plane consisted of seven smaller *y*-*z* cross sections, which were labeled as cs *i*-*j*. *j*=1, 1, 2,…7 was the indexes along y direction.

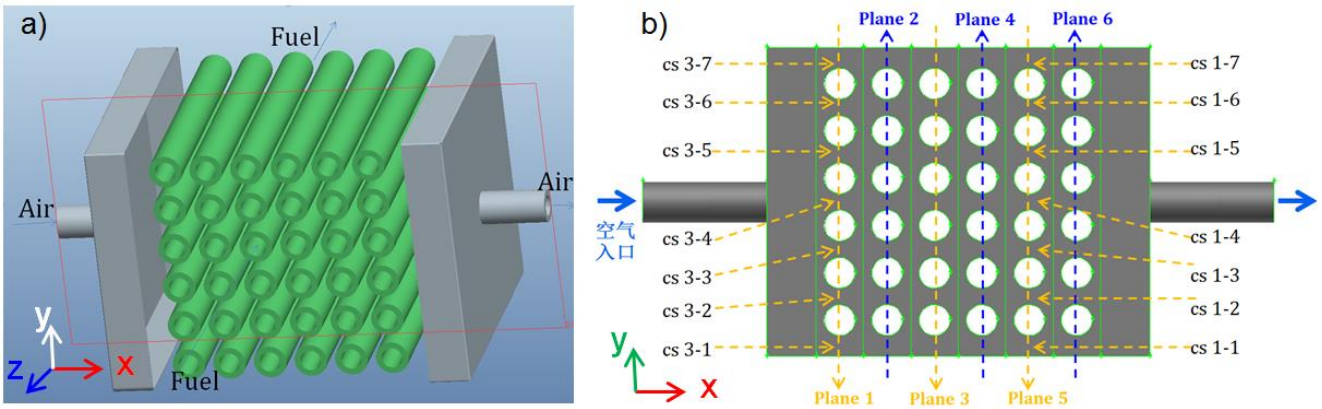

Figure 1. a) Sketch diagram of air flow path within a convenient tubular SOFC stack; b) Indexes of the main planes and cross sections within air flow path.

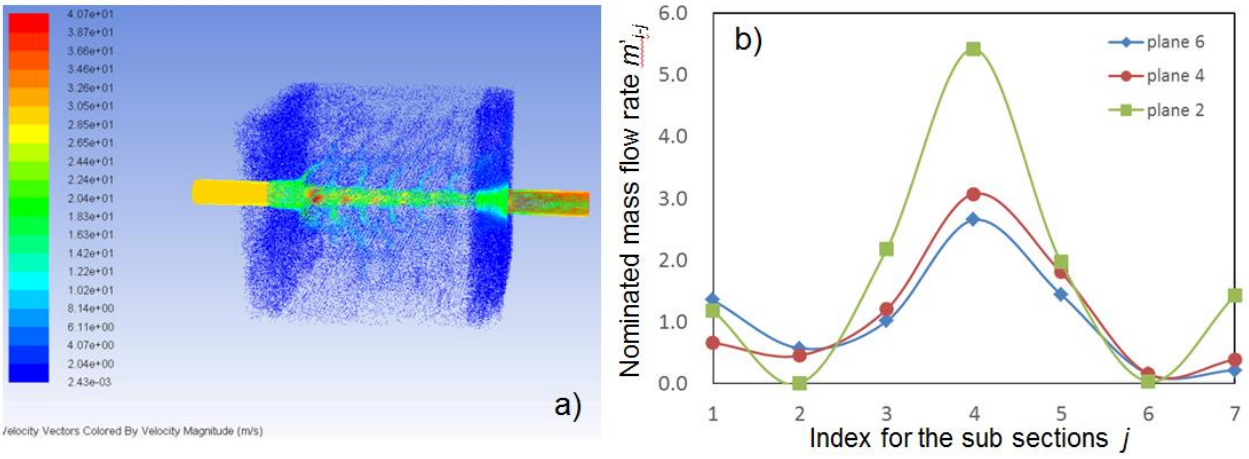

Figure 2. a) 3D velocity vector distributions of particle motion trails within the conventional 1in1out line-type air flow pat； b) the corresponding no-dimensional air mass flow rates through seven sub cross sections of plane *i*=2, 4 and 6, respectively.

3. RESULTS AND DISCUSSION

The air distributing qualities within tubular SOFC stacks could be judged by two levels: i) among 36 T-SOFC units in stack level; ii) over each T-SOFC unit surface in single cell level. Fig. 2a showed the 3D velocity vector distributions of particle motion trails within the conventional 1in1out line-type air flow path design to visually illustrate the movement routes of the air flow particles. Due to its turbulent state, there were obviously vortexes within the stack which was good for uniform distribution of air fluid. However, most of the air flows were concentrated in the middle region due to both the inlet and outlet manifolds were placed at the central positions of the opposite surfaces. Thus, it was reasonable to find that most of the air flow was induced from the inlet manifold and transported out the T-SOFC stack directly.

The corresponding no-dimensional air mass flow rates through seven sub cross sections cs *i-j* of plane *i*=2, 4 and 6 were displayed in Fig. 2b. *i* and *j* were the indexes of the main plane and sub cross section, respectively. The non-dimensional item was used to compare the performances among the T-SOFC stacks with different structure design and working conditions [20, 21],

$$\dot{m}'_{i-j} = \dot{m}_{i-j} / \sum_{k=0}^{6} \dot{m}_{i-k} \text{ , (3)}$$

Where $\dot{m}_{i-j}$ was the air mass flow rate passing through the sub cross section cs *i-j*. The air distribution results in Fig. 2b showed that most of the air flows passed through the sub section cs *i*-4. This could be well consisted with the configuration of air transport process in Fig. 2a in quantity.

Beside the air distribution quality among 36 T-SOFC units, the air flow distributing quality over each T-SOFCs unit surface was another key factor to affect the whole T-SOFC stack performance and its durability life. The detail x-velocity distribution perpendicular to the seven y-z sub cross sections within planes *i*=2, 4 and 6 were pictured out at Fig. 3a, b and c respectively. They could indirectly indicate the air distribution quality over each T-SOFC unit surface. Obviously, there was bad air flow distribution quality over each T-SOFC unit for the conventional air flow path design. The

highest *x*-velocity was appeared at main plane 2 due to it neared the inlet manifold entrance. The x-velocities within plane-6 were distributed more uniformly compared to the other planes, because of far away from the inlet manifold entrance.

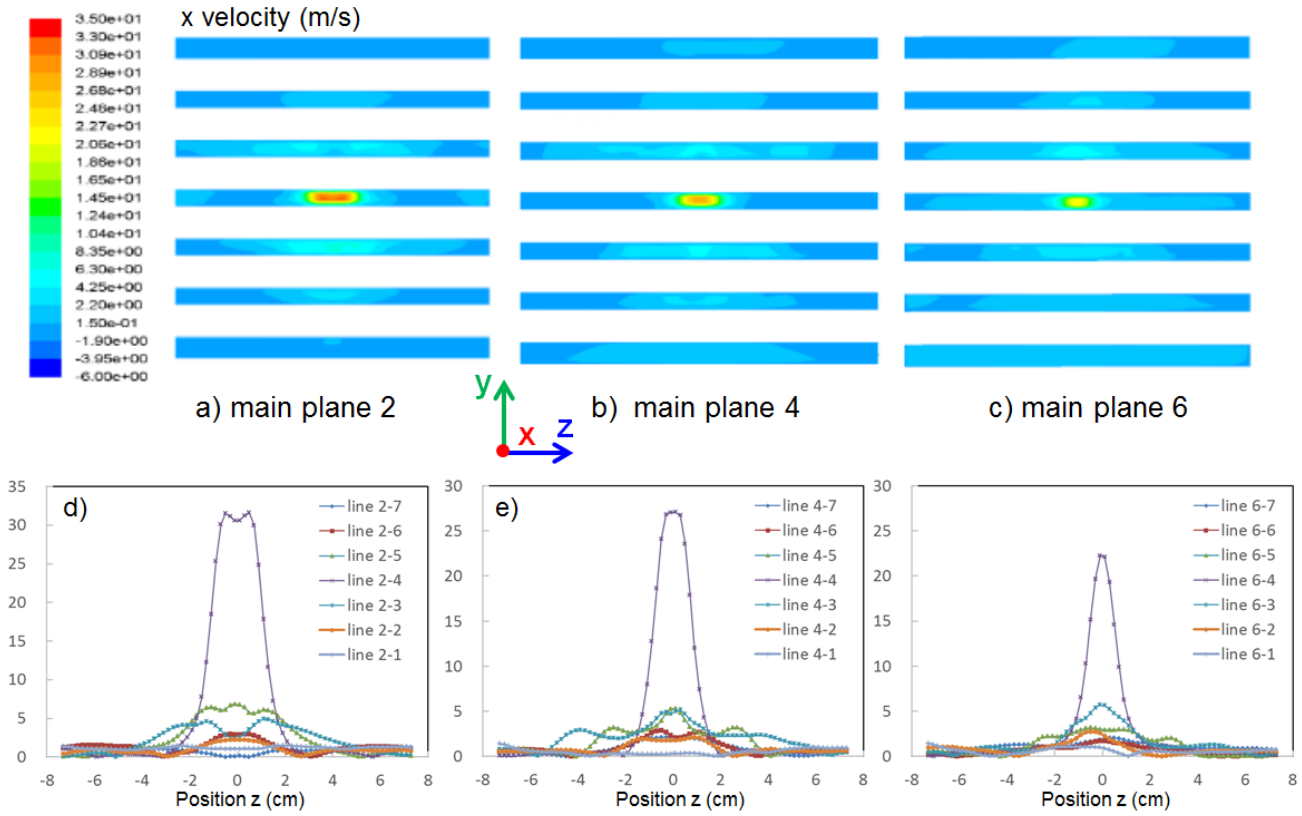

Figure 3. a-c) the detail u_x perpendicular to the seven y-z sub cross sections within planes *i*=2, 4 and 6 for 1in1out line-type air flow path; d-f) The corresponding x-velocities distributions at the center line 'line *i*-*j*' of sub cross section in planes 2, 4 and 6.

The corresponding x-velocities distributions at the center line 'line *i*-*j*' of sub cross section 'cs *i*-*j*' in *i*-plane were curved as Fig. 3d, e and f. Obviously, the peak of the x-velocity were appeared at lines *i*-4 around y=0 positions. The variations of the air flow rate distributions could be estimated by the nominated standard deviations of *x*-velocities over main plane as [18, 21],

$$\sigma_u = \left\{ \frac{\sum_{j=1}^{N} \left(\frac{(u_j - \bar{u})}{\bar{u}} \right)^2}{N} \right\}^{1/2}, \qquad (4)$$

The calculated nominated standard deviations for planes 2, 4 and 6, were 2.06, 2.07 and 1.83, respectively. The results demonstrated that this air flow path structure was impractical, and would lead to greatly reducing of the T-SOFC stack service life. This conclusion could be further supported by the published experiment and review reports [22, 23], thermal cycling was a critical issue for cell durability. For achieving a proper air flow path structure design for T-SOFC stack, air flow distribution

characteristics within two different alternative manifold configuration designs (1in1out-Z type and 2in2out-Z) were analyzed and compared.

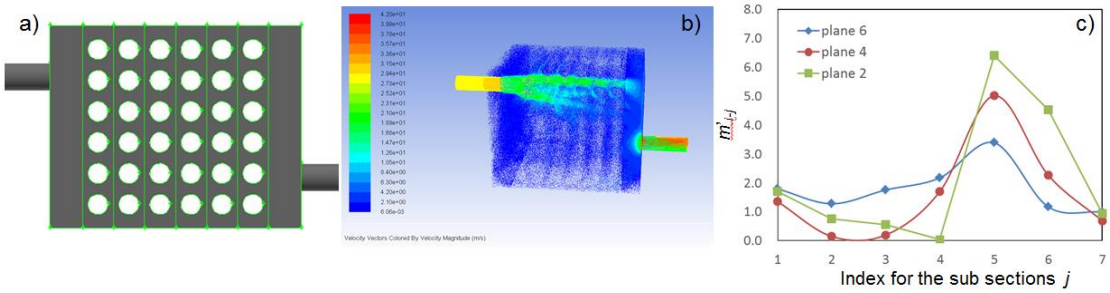

Figure 4. a) sketch diagram of a 1in1out Z-type air flow path configuration; b) the corresponding 3D velocity vector distributions of particle motion trails within it; c) the corresponding no-dimensional air mass flow rates through seven sub cross sections in plane *i*= 2, 4 and 6.

Fig. 4a and b showed the sketch diagram of a 1in1out Z-type air flow path configuration, and the 3D velocity vector distributions of particle motion trails within it to visually illustrate the movement routes of air flow. Obviously, most of the air flow will pass through the top areas of the structure. Fig. 4c showed the corresponding no-dimensional air mass flow rates through seven sub cross section in plane *i*= 2, 4 and 6, respectively. Compared with the conventional 1in1out line-type air flow path, very different air flow distribution trend among the 36 T-SOFC units were obtained. More air flow rates will pass through cs *i*-4, *i*-5 and*i*-6. The air flow distributing quality among 36 piled T-SOFC units was slightly improved.

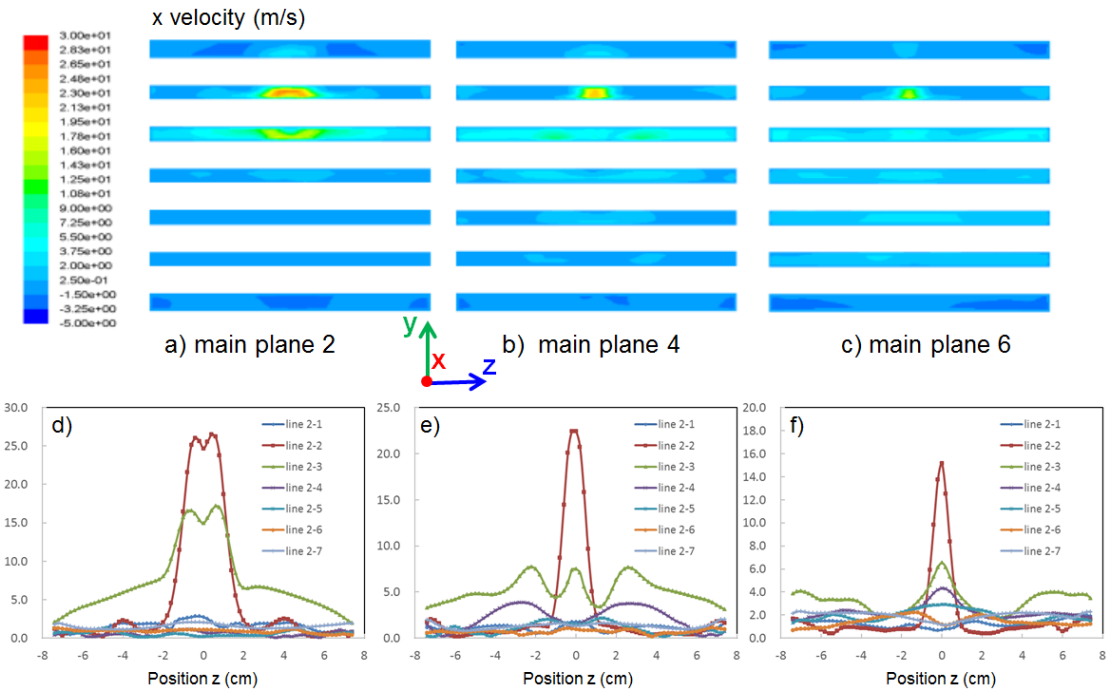

Figure 5. a-c) the detail u_x perpendicular to the seven y-z sub cross sections within planes *i*=2, 4 and 6 for 1in1out Z-type air flow path; d-f) The corresponding x-velocities distributions at the center line 'line *i*-*j*' of sub cross section in planes 2, 4 and 6.

The x-velocity distribution perpendicular to the seven y-z sub cross sections within planes *i*=2, 4 and 6 were pictured out at Fig. 5a, b and c, respectively, to indicate the air distribution quality over each T-SOFC unit surface indirectly. Then, the corresponding horizontal velocities distributions at the center line 'line *i*-*j*' of each sub cross section were figured out as Fig. 5d, e and f. to illustrate the variations of air flow distribution over the relevant T-SOFC unit surface. Compared with that in 1in1out line-type air flow path, the maximum x-velocities within planes 2, 4 and 6 will decrease from 31.6, 27.1 and 22.2 m s^{-1} to 25.4, 21.8 and 14.5 m s^{-1}, respectively. It. meant more air flows would be fed to other places except that around the peak values.

The nominated standard deviations of the *x*-velocities over main plane 2, 4 and 6 were evaluated as 1.819, 1.489 and 0.819, respectively. Obviously, using 1in1out Z-type air flow path configuration could obtained higher air flow distribution quality over T-SOFC unit surfaces than that in 1in1out line-type configuration.

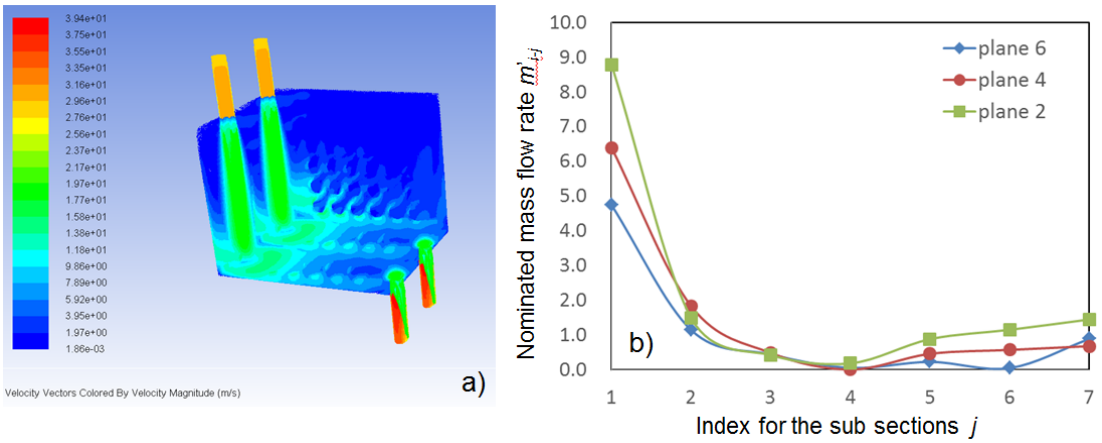

Figure 6. a) 3D velocity vector distribution of particle motion trails within 2in2out Z-type air flow path configuration; b) the no-dimensional air mass flow rates through sub cross sections cs *i*-*j* within three main planes.

Fig. 6 showed the 3D velocity vector distribution of particle motion trails within 2in2out Z-type air flow path configuration to visually illustrate the movement routes of air flow. In this case, most of the air flows were concentrated around the button zone of the stack. Then, the no-dimensional air mass flow rates through sub cross sections cs *i*-*j* within three main planes were displayed in Fig. 6b.As shown in the figure, cs *i*-1 will obtain most of the air flow. Compared with that in conventional 1in1out line-type design, using 2in2out Z-type didn't improve the air flow distribution quality among the 36 T-SOFC units too.

Fig. 7a showed the x-velocity distributions over each seven cross sections within plane *i*=2, 4 and 6, respectively. Then, the corresponding horizontal velocities distributions at the center line 'line i-j' of each sub cross sections were collected in Fig. 7b. Obviously, the air flow distribution quality within this air flow path configuration was greatly improved, compared with that within both the 1in1out line-type and 1in1out Z-type designs. The variations of air flow distribution over the main plane 2, 4, and 6 were statistically counted by the nominated standard deviations of *x*-velocities as

1.016, 1.111 and 1.117, respectively.

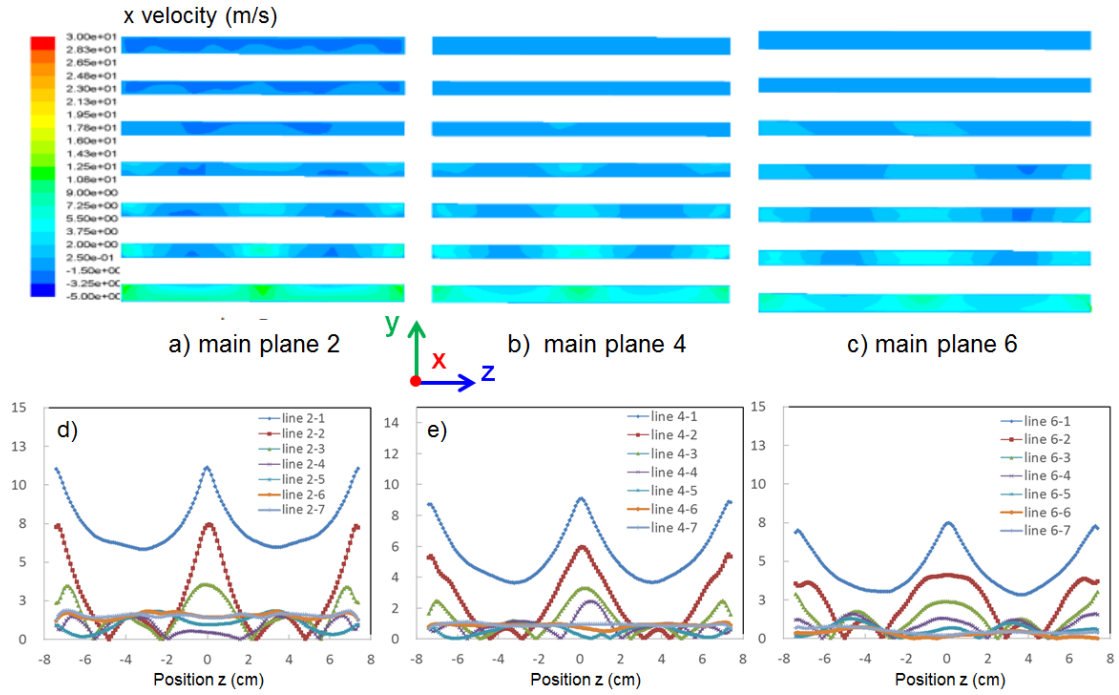

Figure 7. a-c) the detail u_x perpendicular to the seven y-z sub cross sections within planes *i*=2, 4 and 6 for 2in2out Z-type air flow path; d-f) The corresponding x-velocities distributions at the center line 'line *i*-*j*' of sub cross section in planes 2, 4 and 6.

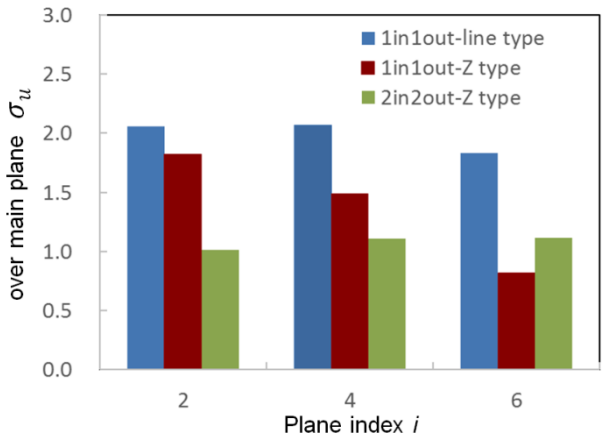

Figure 8. Comparison of the overall nominated standard deviations of *x*-velocities σ_u over plane 2, 4 and 6 among the 1in1out line-type, 1in1out Z-type and 2in2out Z-type air flow path structures using in T-SOFC stacks were compared.

As shown in Fig. 8 the overall nominated standard deviations of *x*-velocities three plane 2, 4 and 6, which indicated the air flow distribution quality over each T-SOFC unit surface, were quite different among the 1in1out line-type, 1in1out Z-type and 2in2out Z-type air flow path structures. 2in2out Z-type air flow path configuration was considered to be a better choose than the other two

different configurations, due to the relevant lower variations of x-velocity over the surfaces of each T-SOFC units.

4. CONCLUSIONS

In this study, the 3D CFD analyzing model for the 1in1out line-type air flow path within a conventional T-SOFC stack had been well developed to figure out the flow distribution characteristics. The air fluid transport process within the structure was found to be a typical turbulence flow. T-SOFC stack with 2in2out Z-type manifold configuration would lead to a great improvement of the air flow distributing uniformity over each T-SOFCs unit surface in single cell level. It was concluded to be a more suitable air flow path design for the typical T-SOFC stacks. However, it should also be mentioned that compared with the conventional 1in1out line-type manifold configuration, not matter using 1in1out Z-type or 2in2out Z-type designs could not apparently improved air flow distributing quality among 36 T-SOFC units. The air flow distribution quality in stack level should be further concerned and improved by some other alternative air flow path configurations in the near future.

ACKNOWLEDGEMENTS
We gratefully acknowledge the financial support of the National Science Foundation of China 21106058, the Jiangsu Province Colleges and Universities Natural Science Projects (13KJB480003).

References

1. D. Chen, Q. Zhang, L. Lu, V. Periasamy, M.O. Tade, Z. Shao, *J Power Sources*, 303 (2016) 305-316.
2. Xiang Gao, Qiang Zhang, Wenxuan Zhang, D. Chen, *Int. J. Electrochem. Sci.*, 10 (2015) 7521-7534.
3. Wei Kong, Wenxuan Zhang, Shundong Zhang, Qiang Zhang, S. Su, *International Journal of Hydrogen Energy*, (2016).
4. M. Peksen, *International Journal of Hydrogen Energy*, 39 (2014) 5137-5147.
5. P. Batfalsky, J. Malzbender, N.H. Menzler, *International Journal of Hydrogen Energy*, 41 (2016) 11399-11411.
6. L. Jin, W. Guan, J. Niu, X. Ma, W.G. Wang, *J Power Sources*, 240 (2013) 796-805.
7. L. Blum, H.P. Buchkremer, S. Gross, A. Gubner, L.G.J. de Haart, H. Nabielek, W.J. Quadakkers, U. Reisgen, M.J. Smith, R. Steinberger-Wilckens, R.W. Steinbrech, F. Tietz, I.C. Vinke, *Fuel Cells*, 7 (2007) 204-210.
8. W.S. Xia, Y.Z. Yang, Q.S. Wang, *J Power Sources,* 194 (2009) 886-898.
9. D. Chen, H. Wang, S. Zhang, M.O. Tade, Z. Shao, H. Chen, *Aiche Journal,* 61 (2015) 3786-3803.
10. D. Chen, H. He, D. Zhang, H. Wang, M. Ni, *Energies,* 6 (2013) 1632-1656.
11. L. Lu, D. Chen, G. Zhao, X. Ren, G. Guo, The *Journal of Physical Chemistry* C, 114 (2010) 18435-18438.
12. Wei Kong, Xiang Gao, Shixue Liu, S. Su, a.D. Chen, *Energies* 7(2014) 295-313.
13. M. Peksen, R. Peters, L. Blum, D. Stolten, *International Journal of Hydrogen Energy*, 36 (2011) 6851-6861.

14. Y.-P. Chyou, T.-D. Chung, J.-S. Chen, R.-F. Shie, *J Power Sources*, 139 (2005) 126-140.
15. C.M. Huang, S.S. Shy, H.H. Li, C.H. Lee, *J Power Sources*, 195 (2010) 6280-6286.
16. D. Yan, Z. Bin, D. Fang, J. Luo, X. Wang, J. Pu, B. Chi, L. Jian, Y. Zhang, *International Journal of Hydrogen Energy*, 38 (2013) 660-666.
17. P.W. Li, S.P. Chen, M.K. Chyu, *J Power Sources,* 140 (2005) 311-318.
18. S. Su, H. He, D. Chen, W. Zhu, Y. Wu, W. Kong, B. Wang, L. Lu, *International Journal of Hydrogen Energy*, 40 (2015) 577-592.
19. B. Timurkutluk, C. Timurkutluk, M..Mat, Y. Kaplan, *Renewable and Sustainable Energy Reviews*, 56(2016) 1101–1121.
20. D. Chen, Q. Zeng, S. Su, W. Bi, Z. Ren, *Appl Energ*, 112 (2013) 1100-1107.
21. K. Rashid, S. K. Dong, R. A. Khan, S. H. Park, *Journal of Power Sources*, 327(2016) 638-652.
22. K. S. Howe, G. J. Thompson, K. Kendall, *Journal of Power Sources*, 196(2011) 1677-1686.
23. V. Lawlor, S. Griesser, G. Buchinger, A.G. Olabi, S. Cordiner, D. Meissner, *Journal of Power Sources*, 193(2009) 387-399.